RESEARCH

Does Adsorption of Cd, Cu and Pb on Polymeric Silicic Acid Occur Under Acidic Conditions?

Mathias Stein[1,2] · Maria Buchweitz[3,4] · Pia Mayer[3,5] · Thilo Rennert[1]

Abstract

Contamination with Cd, Cu and Pb is a major environmental issue. Cations of those metals may adsorb on negatively charged surfaces of polymeric silicic acid (pSi), altering their environmental fate. Aiming to elucidate the underlying mechanisms and the extent of adsorption, we conducted batch adsorption experiments at pH 4 to 6 and concentrations that excluded precipitation of solid phases. Zeta-potential measurements were conducted to monitor surface charge changes. In addition, isothermal titration calorimetry (ITC) was used to derive thermodynamic parameters of the interaction between the metals and pSi. Surprisingly, neither did batch-adsorption experiments reveal any metal adsorption on pSi after 24 h reaction time, nor did ITC experiments show any evidence for chemical adsorption of the metals, as no heat was released or absorbed during the experiments. However, zeta-potential measurements indicated weak electrostatic interactions between the negatively charged silanol groups and the metals. These electrostatic interactions may be the initial step of metal incorporation into the matrix of polymerizing silicic acid, which were spectroscopically proven in long-term experiments.

Keywords Potentially toxic elements · Isothermal titration calorimetry · Electrostatic interactions · Zeta potential

1 Introduction

Soil and water contamination with potentially toxic elements (PTEs) has become a serious problem for ecosystem functioning [1]. Most recently, the potential of silicon (Si) to decrease the mobility of PTEs such as Cd, Cu, and Pb in the environment was found [2].

Silicon, the second-most abundant element in the earth's crust (elemental content 28.8 mass-%) [3], occurs in most primary minerals such as feldspars, micas, and quartz as well as in secondary clay minerals, and as amorphous Si (ASi), either biogenic (e.g., as phytholite) and minerogenic [4]. Dissolved Si species in the environment comprise monomeric silicic acid (mSi), an isolated molecule (H_4SiO_4) and its polymers, designated as polymeric silicic acid (pSi). Mineral weathering and dissolution control the release of mSi and pSi into solution [5]. Total Si concentrations in soil solutions range from 0.4 to 2000 μmol L^{-1}, mostly between 100 and 500 μmol L^{-1} [6]. In early stages of weathering ∼50 mol-% of total dissolved silicic acid might be in the form of pSi [4]. Polymerization and depolymerization of silicic acid control Si availability and transport in soils. These processes depend on the chemical composition of the solution and are mainly driven by its initial silicic acid concentration, pH, and ionic strength [5]. Polymerization of silicic acid increases from pH 3 to 6, has its maximum at pH 7 to 8, and decreases at more alkaline pH [4, 7]. The reaction releases molecular water and forms dimers, trimers, oligomers, and finally nano-particulate pSi bearing negative surface charge [8]. In contrast, mSi may be uncharged at pH 2 to 7 [7]. In pure water and at room temperature, mSi polymerizes at c > 1 mM, but at alkaline pH and increasing temperature, its solubility increases as polymerization decreases [4]. Additionally, cations such as Na$^+$, K$^+$, Ca^{2+}, Mg^{2+}, Pb^{2+}, Cu^{2+}, and Cd^{2+} decreased the solubility

✉ Mathias Stein
mathias.stein@zalf.de

[1] Department of Soil Chemistry and Pedology, Institute of Soil Science and Land Evaluation, University of Hohenheim, 70593 Stuttgart, Germany

[2] Working Group Silicon Biogeochemistry, Leibniz Centre for Agricultural Landscape Research (ZALF), 15374 Müncheberg, Germany

[3] Department of Food Chemistry, Institute of Biochemistry and Technical Biochemistry, University of Stuttgart, 70569 Stuttgart, Germany

[4] Department of Chemistry, Institute of Food Chemistry, University of Hamburg, 20146 Hamburg, Germany

[5] Department of Food Science, University of Copenhagen, Frederiksberg 1958, Denmark

of mSi by favouring its polymerization [2, 5]. It is assumed that monomeric silicic acid protonates at pH < 2, forming cationic $Si(OH_2)^+$, and at pH > 7, the weakly acidic silanol group deprotonates, forming an anion $Si(OH)_3O^-$ [7]. Dissolved Si adsorbs reversibly on Fe and Al oxides/hydroxides whereby pSi has a higher affinity than mSi. Thus, mSi is the dominant species in the soil solution [4]. Polymeric silicic acid depolymerizes after adsorption on soil constituents, releasing mSi into the soil solution [5]. At very acidic pH (< 3.6), silicic acid may precipitate on surfaces of soil constituents forming minerogenic ASi coatings [9] from which mSi is released in solution as desorption of mSi is favoured at decreasing pH [5].

Interactions between silicic acid and PTEs such as Cd, Cu, and Pb comprise various processes that may contribute to the mobility of these PTEs in the environment. Some studies [e.g., 10–12] suggest metal adsorption on the weakly acidic silanol group ($pK_a = 7.2$) on the pSi surface, assuming ion exchange between H^+ and the metal cations. Generally, the adsorption of metal cations on pSi increases with increasing pH, as deprotonation of the silanol group also increases with increasing pH [7, 12]. Consequently, adsorption of Zn^{2+}, Ni^{2+}, and Cd^{2+} on pSi surfaces increased with increasing pH. Moreover, adsorption increased with increasing temperature and ionic strength of the solution [13]. Adsorption kinetics may depend on ion hydrolysis, as strongly hydrolysed ions may adsorb more slowly than non-hydrolysed ions [14]. Copper adsorption on silica surfaces was modelled to occur already close to the point of zero charge, but Cu may also precipitate as $Cu(OH)_2$ on pSi surfaces, even at low concentrations [15, 16]. As mSi is uncharged between pH 2 and 7 [7], Cu may not interact with mSi in this range of pH. Applying the Poisson-Boltzmann equation on published data, Pivovarov (2010) reported that especially Cd adsorption on silicic acid is electrostatic [17]. Flow microcalorimetry analyses also indicated that interactions between Cd and pSi surfaces may be mainly electrostatic, as the heat of Cd adsorption was negligibly low [18]. Coagulation experiments with pSi and Cu showed increasing interactions between pSi and Cu between pH 5.5 and 7, followed by a sharp decrease from pH 7.25 to 7.5 [19]. Thus, the affinity of Cu for silicic acid increased with its increasing polymerization.

However, most experiments were conducted at pH ≥ 6 [e.g., 11, 15, 16], high background electrolyte concentration [12], temperature above ambient conditions [13], and with silanized or functionalised precipitated silicic acid [14]. In some studies [e.g., 13], precipitation of minerals was excluded because of initial Si and metal concentration, while other studies did not check the possibility of precipitation [e.g., 11]. In a study on the interactions between Cu and Cd and silicic acid at initial concentrations that excluded mineral precipitation, Cu was structurally incorporated into the polymeric network of pSi or formed inner-sphere complexes,

while Cd formed weaker outer-sphere complexes [2]. Nonetheless, their experimental approach excluded the quantification of metal adsorption. Stein et al. (2021) showed that interactions of silicic acid with Cd^{2+} and Cu^{2+} under acidic conditions were not restricted to the aqueous phase, as they occurred in soil as well. Potential processes detected in long-term experiments (up to 211 days) included adsorption on external surfaces, diffusion/occlusion of the metals in the interior of polymerizing silicic acid, and structural incorporation [20]. The precondition of these processes expressed in the long-term is that Cd^{2+}, Cu^{2+}, and Pb^{2+} have interacted with pSi surfaces at acidic pH (4–6) by adsorption, that is, at low concentrations that prevented mineral precipitation. Therefore, the objective of this study was to elucidate the extent and the mechanisms of the adsorption of Cd^{2+}, Cu^{2+}, and Pb^{2+} on pSi under these experimental conditions. We focussed on adsorption on pSi, as mSi is uncharged at pH 4–6, which excludes electrostatic attraction of the cations, and when mSi tends to polymerize to pSi. We hypothesised that adsorption of divalent Cd, Cu and Pb cations on pSi occurs under acidic conditions (i) and increases with increasing pH (ii). Hence, we conducted batch experiments to quantify metal adsorption on pSi, which bears negative charge at pH 4–6. In terms of mechanistic interpretation of the possible adsorption processes, we determined the surface charge (zeta potential) before and after the batch experiments and used isothermal titration calorimetry (ITC) to derive the thermodynamic parameters ΔH (enthalpy), ΔS (entropy), binding affinity, and the stoichiometry [21] of the interaction between the metals and pSi.

2 Materials and Methods

2.1 Synthesis of pSi from mSi

Polymeric silicic acid was synthesized at ambient temperature and pressure using a 10 mmol tetraethyl orthosilicate solution (TEOS; p.a. grade, Merck, Darmstadt, Germany), which hydrolyses to mSi and ethanol in aqueous solution (Belton et al., 2012). The mSi solution (pH 5.8–6.0) was allowed to polymerize for 211 days. Residual mSi was removed from the pSi suspension by dialysis using a chemically pre-treated regenerated cellulose membrane with a molecular weight cut-off of 1000 Da (Spectra/Por 7, Repligen, Rancho Dominguez, USA). We freeze-dried the dialyzed pSi to obtain a porous cryogel for the batch experiments and characterization. For batch-adsorption experiments, we dispersed the cryogel in deionised water (3 g L^{-1}) and used it as stock suspension.

For microcalorimetry, pSi was synthesized using 10 mmol TEOS. After hydrolysis, the solution was allowed to polymerize for 60 days, and subsequently dialysed.

2.2 Physical and Structural Characterization of pSi

The specific surface area (SSA) was derived by the Brunauer-Emmet-Teller (BET) equation after N_2 adsorption and desorption at 77 K using a Quantachrome Autosorb iQ (Anton Paar Quanta Tec Inc., USA). The samples were degassed prior to analysis for 8 h at 60 °C. Particle charge (zeta potential), particle-size distribution and the intensity weighted mean hydrodynamic diameter (z-average) of pSi were measured before and after the batch experiments using a Zetasizer Nano ZSP (Malvern Panalytical, Herrenberg, Germany) equipped with a He-Ne laser ($\lambda = 633$ nm) and a non-invasive backscatter detector at a fixed angle of 173°.

The structure of the freeze-dried pSi was analysed using transmission Fourier transform infrared (FTIR) spectroscopy. 120 spectra were collected in the range of 4000 to 500 cm^{-1} at a resolution of 4 cm^{-1} using the transmission accessory of a LUMOS infrared microscope (Bruker, Ettlingen, Germany). Prior to analysis, the sample was ground in an agate mortar together with KBr (1 mg pSi and 400 mg KBr) and pressed into pellets.

2.3 Batch-Adsorption Experiments

Batch experiments were conducted at initial pH 4 and 5 with all metals and additionally at pH 6 with Cd, and 24 h contact time at ambient temperature. The experiments were performed in triplicate at a solid to solution ratio of 1:200. We prepared a pSi stock suspension (3 g L^{-1}) and metal stock solutions (20 mmol L^{-1} as their nitrate salts (Cu $(NO_3)_2 \times 3H_2O$ (ACS grade, ABCR, Karlsruhe, Germany), Cd $(NO_3)_2 \times 4H_2O$ (Puratronic, ABCR) and Pb $(NO_3)_2$ (ACS grade, ABCR)). The pH was adjusted in both the pSi suspension and the metal solutions by dropwise adding dilute NaOH (AppliChem GmbH, Darmstadt, Germany) or HCl (Chemsolute, Th. Geyer GmbH & Co. KG, Renningen, Germany), respectively. Ten mL of the pSi stock suspension were pipetted into 25 mL polycarbonate bottles. Subsequently, varying amounts of the metal stock solutions were added resulting in initial concentrations of 2, 4, 6, 8 and 10 mmol L^{-1} and a final volume of 25 mL. Samples were shaken at 20 rpm using an over-head shaker (GFL 3040, Burgwedel, Germany). Subsequent phase separation was conducted using an ultra-centrifuge (Beckman Coulter, Krefeld, Germany) at 300,000 g to ensure complete separation of pSi. Metal and Si concentrations in the supernatants were measured by inductively coupled plasma optical emission spectrometry (ICP-OES, Horiba Ultima 2, Kyoto, Japan) using their most sensitive atomic bands. The detection limits (DL) of the metals under study were 0.019 μmol L^{-1} for Cu, 0.0059 μmol L^{-1} for Cd, and 0.016 μmol L^{-1} for Pb. In addition, the pH was measured before and after the experiments, as proton release upon adsorption is known for metal binding on silanol groups [12].

2.4 Microcalorimetric Study

Thermograms of the reaction (heat flux as a function of time) between pSi and Me^{2+} were obtained in an isothermal titration calorimeter (Affinity ITC, TA Waters, New Castle, USA) at 25 °C by multiple-injection and single-injection measurements. We set the pH to 4.6, similar to the batch-adsorption experiments. For the multiple-injection measurements, 30 injections of 3 μL of a 50 mmol Cu$(NO_3)_2$ or Cd$(NO_3)_2$ solution were added into the sample cell containing 182 μL of a 10 mmol pSi suspension. The metal concentration in the sample cell increased by 0.81 mmol with each injection, resulting in a final metal concentration of 16.36 mmol. Every injection was followed by 200 s delay time allowing the baseline to return to equilibrium. Heat effects of dilution (enthalpy of mixing) of the metal nitrates were assessed by blank experiments. Blanks were determined by titrating the metal solutions into deionised water with the same pH using the same procedure as described above. For single-injection experiments, a single volume of 10 μL of a 50 mmol Cu$(NO_3)_2$ solution was titrated into 182 μL of a 10 mmol pSi suspension resulting in a metal concentration of 2.74 mmol in the sample cell and a decrease in Si concentration by 0.67 mmol. The heat rate was monitored for 60 h after the injection. Each experiment was at least duplicated, and all samples were degassed prior to the experiment.

3 Results and Discussion

3.1 Physical and Structural pSi Characteristics

Transmission FTIR spectra of the pSi (Fig. 1) revealed absorption bands of -OH bending close to 3450 cm^{-1}. These groups are part of water molecules and of silanol groups (Si-OH), which are mostly located on the surfaces of pSi [22]. The band at 955 cm^{-1} is also characteristic of silanol groups (Si-O stretching vibration). The most important spectral region for Si at 1111 cm^{-1} is attributed to asymmetric stretching vibrations of Si-O-Si. Broadening of this band is caused by lower internal order of the Si structure [2, 22]. The narrow shape of the band indicates high internal order. Signals observed at 790 cm^{-1} are attributed to symmetrical Si-O stretching vibrations [22]. Infrared spectra of the material under study correspond to those of ASi phases (e.g., precipitated silicic acid and pyrogenic silica) [22].

The SSA of pSi was 550 m^2 g^{-1}, which exceeds that of other ASi samples studied, 14.29 to 431.4 m^2 g^{-1} [23]. The larger surface may be explained with the small particle size (45 nm) of the pSi measured in solution before freeze-drying. The zeta potential at pH 6 was -26.3 mV, which is more negative than that of other ASi nanoparticles at pH 6 [24, 25].
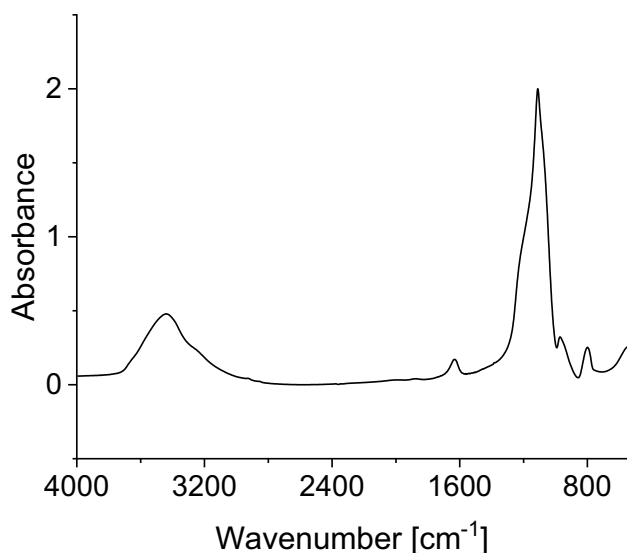
Fig. 1 Fourier transform infrared spectra of freeze-dried polymeric silicic acid, produced from 10 mmol tetraethyl orthosilicate

3.2 Batch-Adsorption Experiments

In contrast to our expectations that were based on published studies [e.g., 10–12], the batch experiments did not reveal any adsorption of Cd^{2+}, Cu^{2+}, and Pb^{2+} on pSi at pH 4 to 6 and after 24 h reaction time, as the concentrations in the supernatants after the experiments equalled the initial ones. Considering the DLs of metal analysis, the minimum detectable metal adsorption would have been 0.042 µmol Me^{2+} g^{-1} pSi. Furthermore, no dissolved Si was present in the supernatants, indicating complete separation of pSi and no depolymerization of mSi from pSi. Divalent cations such as Cd^{2+}, Cu^{2+} and Pb^{2+} promote the polymerization of silicic acid [2] and thus, may stabilize pSi against depolymerization. Additionally, no Si was found in the supernatants of the control samples confirming that depolymerization of pSi is a slow process not occurring within 24 h under the experimental conditions.

Our findings do not fully support previous research, where adsorption of divalent cations on silica surfaces was detected [e.g., 11–14]. This discrepancy can be attributed to differences in experimental conditions especially pH, ionic strength, type of adsorbent (e.g., functionalized or acidified ASi), adsorbent concentration, and temperature. The previous studies were conducted at pH > 6, where silanol groups are increasingly deprotonated, providing more negative surface charge. Besides determining the physicochemical properties of silicic acid, the pH has a strong influence on the speciation and thus solubility of the metals. The solubility of the metals decreases with increasing pH as they precipitate in solution [26] or on mineral surfaces [27], or both. Moreover, metals are preferentially adsorbed in their $MeOH^+$ state, which also increases with increasing pH [27]. Thus, at pH > 6, the removal of the
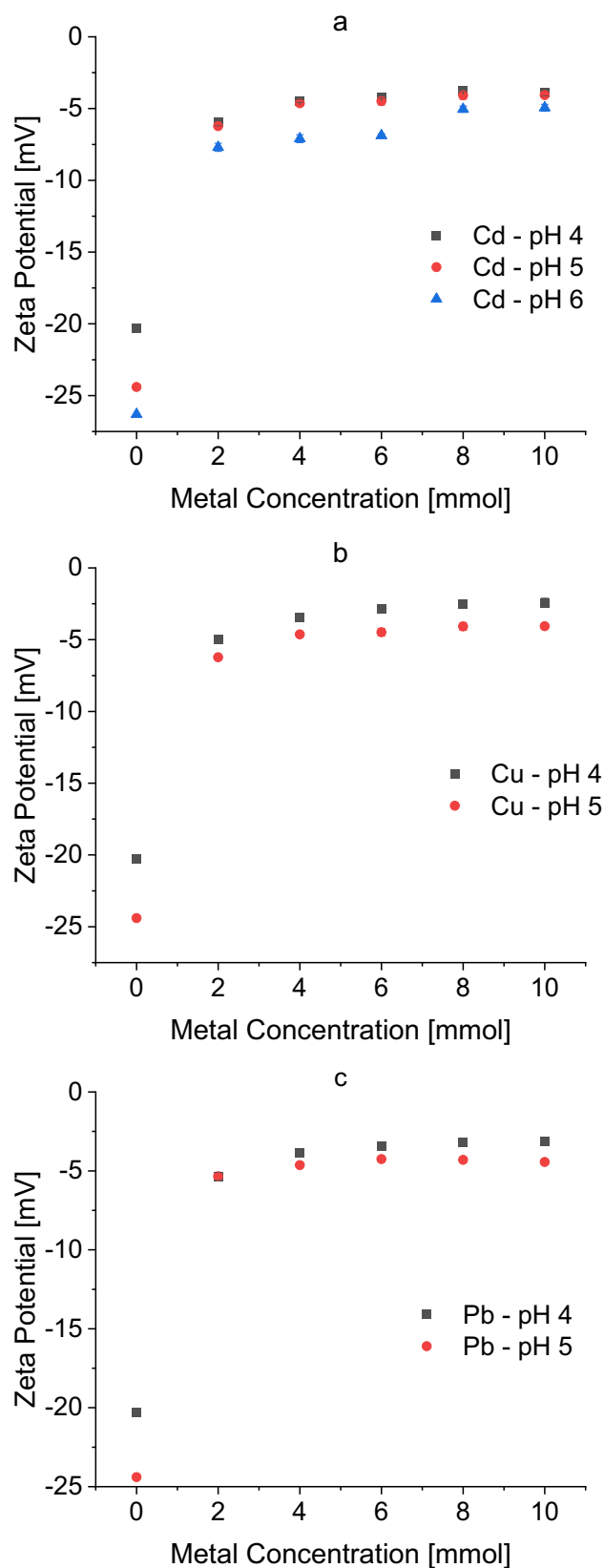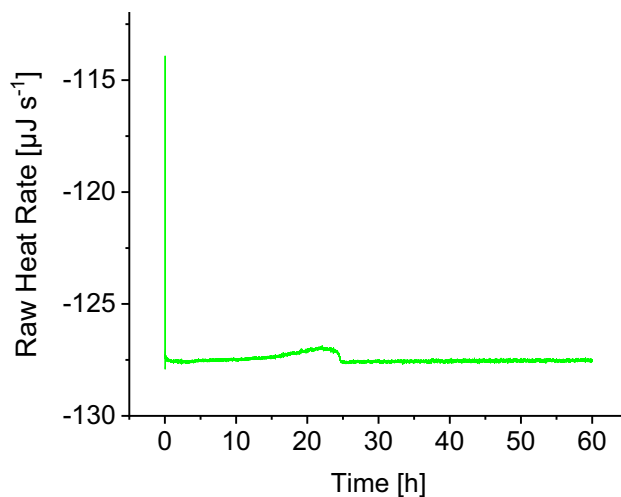

Fig. 2 Zeta potentials as a function of initial metal concentrations in batch experiments with polymeric silicic acid and **a** Cd, **b** Cu, and **c** Pb
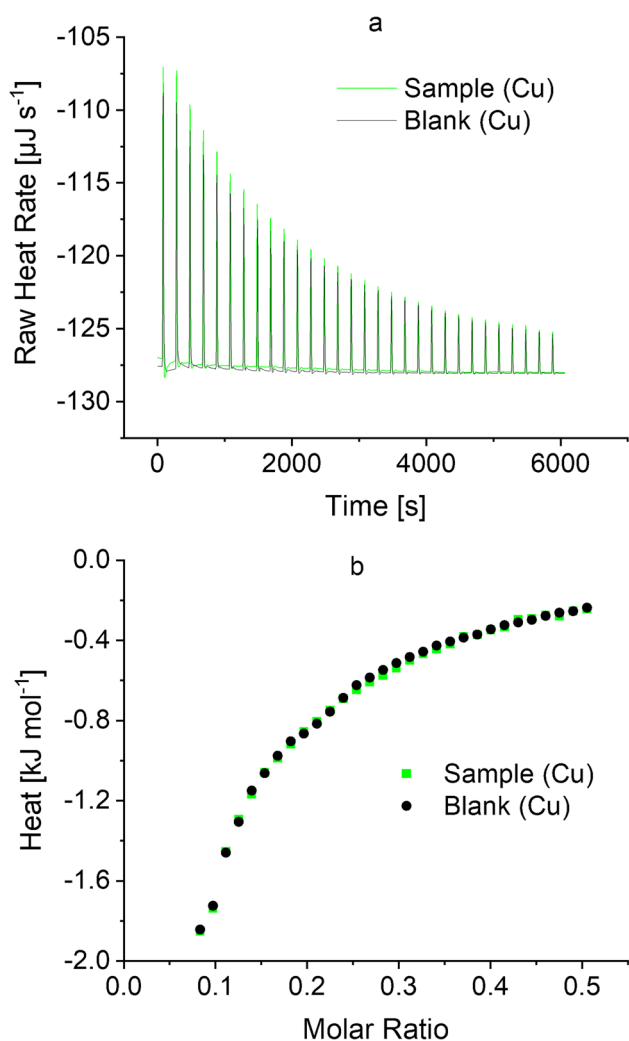
Fig. 3 Thermograms (heat rate as a function of time) of the interaction between 10 mmol polymeric silicic acid and $Cu(NO_3)_2$ derived from multi-injection experiments using isothermal titration calorimetry (**a**), and **b** the integrated heat pulses, normalized per mol of $Cu(NO_3)_2$ as a function of the molar ratio

Fig. 4 Thermogram (heat rate as a function of time) of the interaction between 10 mmol polymeric silicic acid and $Cu(NO_3)_2$ derived from single-injection experiments using isothermal titration calorimetry

metals by adsorption of divalent cations may be of minor importance. More likely, the decrease of metal concentration observed in other studies (e.g., [11]), may be attributed to precipitation of the metals. To test this hypothesis, we calculated the chemical speciation based on published data using Visual MINTEQ 3.0) [28]. In this study [11], Zn was oversaturated with respect to precipitation of $Zn_5(OH)_8Cl_2$ reducing both, Zn^{2+} and OH^- concentration in the solution. Thus, a decrease in solution pH, which was attributed to ion exchange between H^+ and the divalent metal cations [11], could also be explained by consumption of OH^-. In our study, the geochemical speciation was calculated using Visual MINTEQ 3.0 to exclude precipitation of minerals especially silicates and hydroxides under the used experimental conditions. In addition to pH, controlling the interactions between silicic acid and the metals,

temperature has an influence on metal adsorption too. Mustafa et al. (2003) showed that the adsorption of divalent cations on pSi at pH 5 strongly increased with temperature in the range of 30–50 °C [13]. Copper ions were not adsorbed on pSi at pH < 5 and pH > 8 [19]. In long-term experiments in acidic aqueous solution, Cd^{2+}, Cu^{2+}, and Pb^{2+} did not interact with silicic acid within 35 days, as it was predominantly present as mSi [2], which was also shown by Yates et al. (1998) for Cu^{2+} [19]. Then, the PTEs successively interacted with the progressively polymerizing silicic acid [2, 19]. However, pSi bound only traces of the metals [2].

Even though the batch experiments revealed no metal adsorption within 24 h, zeta potentials of the pSi decreased in the course the experiment (Fig. 2). The initial zeta potentials increased with increasing pH, -20.3 mV at pH 4, -24.4 at pH 5 and −26.3 mV at pH 6. This pH dependency is common with Si nanoparticles [24, 25] and explained by progressive deprotonation of the silanol groups with increasing pH [7]. Absolute zeta potentials decreased from < -20 mV to > -3 mV (pH 4) with increasing metal concentration and slightly differed between the metals (Fig. 2). The decrease was most pronounced for Cu and least for Pb, as the effect on the decrease of the zeta potential increases with decreasing ion size of the counter ion, since physical accessibility increases with decreasing hydrated ionic diameter (here Pb, 0.882 nm > Cd, 0.852 nm > Cu, 0.838 nm, [29]). Furthermore, short-range repulsion is decreased with decreasing size of the hydrated ion [30, 31]. Thus, smaller ions are attracted more strongly, consequently increasing shielding of the negative surface charge. In general, changes in zeta potential by counter-ion shielding of the negatively charged silanol groups have different reasons. First, the cations are adsorbed within the Outer Helmholtz plane (OHP), which is excluded in our study because of the lack of adsorption in batch

experiments. Second, ions in the diffuse double layer (DDL) leading to its compression, consequently decreasing the magnitude of the zeta potential [32]. Third, as cations are electrostatically attracted by negative surface charges, they accumulate in the DDL and the shear plane. These electrostatic interactions were described particularly for Cd in previous studies [17, 18]. Thus, divalent metal cations alter the charge of the silanol surfaces without forming inner spherical bonds with these surface groups. However, zeta potential measurements cannot be used to quantify the adsorption of metals like Cu on charged surfaces [33]. Nevertheless, it may be a simple measure to access the adsorption ability of charged colloidal particles [34].

Besides providing information about the surface charge of pSi, the zeta potential is a main indicator for the stability of colloidal dispersions. The higher its absolute value, the stronger is the electrostatic repulsion and the more stable the dispersion [35]. In that study, Cd, Cu, and Pb cations decreased the zeta potential and consequently decreased the stability of the colloidal pSi dispersion. Hence, attractive forces may prevail, and aggregation occurs resulting in larger units of pSi. The results of our study may be interpreted as the initial step of the long-term interactions between Cd^{2+}, Cu^{2+}, and Pb^{2+} and (polymerizing) silicic acid, which were spectroscopically proven [2]. The accumulation of the metals in the shear plane of the DDL by electrostatic forces may foster inner-sphere complexation. Especially Cu was structurally incorporated during the polymerization of silicic acid

or formed inner-sphere complexes with deprotonated silanol groups [2]. The waning effect of Cd^{2+}, Cu^{2+}, and Pb^{2+} on the zeta potential may promote polymerization of silicic acid [2]. However, these processes are slower than adsorptive interactions with other soil constituents and may not be predicted by thermodynamic equilibrium [4, 20]. Furthermore, only traces of the metals were bound in the long-term experiments, which also accords with the current study, with no adsorption in the batch experiments within 24 h.

3.3 Microcalorimetric Study

We conducted ITC to assess thermodynamic parameters of the interaction between silicic acid and Cu^{2+} and Cd^{2+}. Figure 3a shows the thermogram (heat rate as a function of time) for 10 mmol polymeric silicic acid and $Cu(NO_3)_2$ in multi-injection experiments. To improve visual comparability of the data, the integrated heat pulses, normalized per mol of $Cu(NO_3)_2$ as a function of the molar ratio are shown in Fig. 3b. The heat rates showed, besides a slightly higher baseline, no difference to the blank measurement, that is, $Cu(NO_3)_2$ titrated into deionized water. Thus, no heat was released (exothermal process) or absorbed (endothermic process). Consequently, we did not detect any difference in integrated heat pulses, normalized per mol of $Cu(NO_3)_2$ (Fig. 3b). Similar results were observed for Cd (data not shown). In accordance with our study, Lantenois
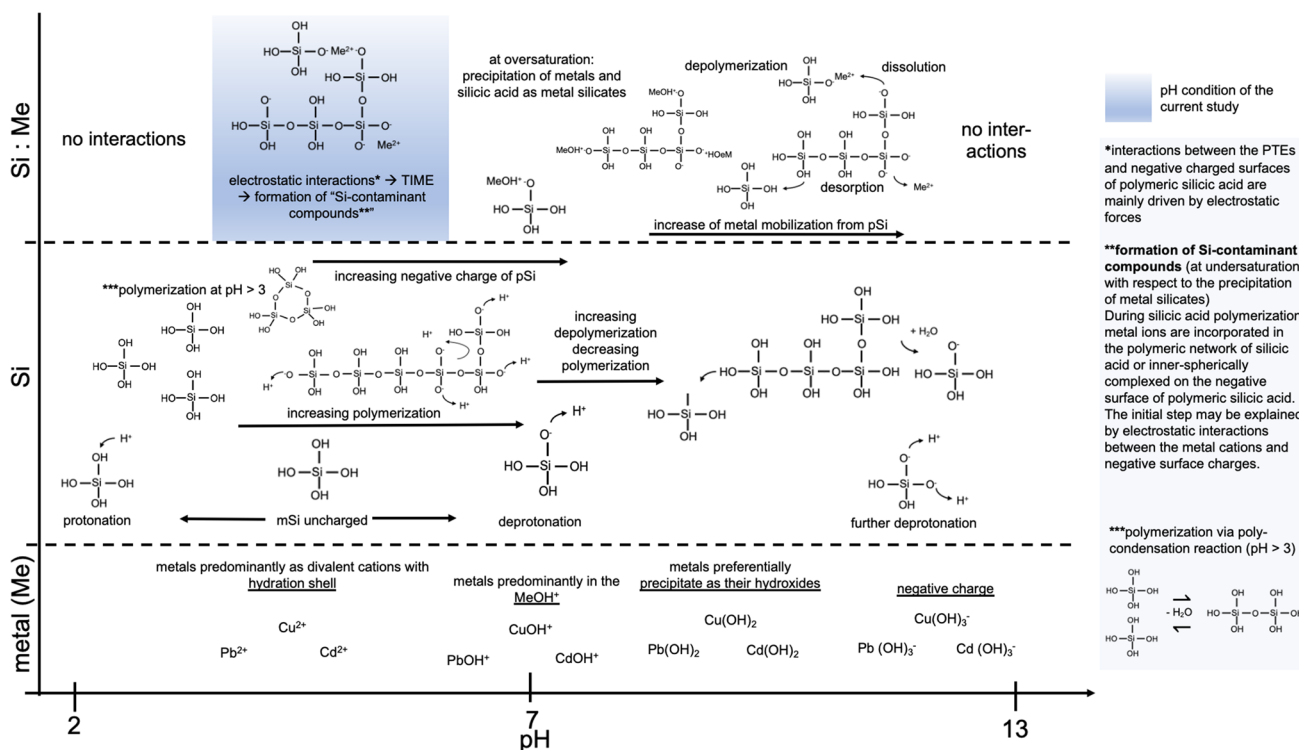

Fig. 5 Potential interactions of silicic acid and Cd, Cu, and Pb, depending on pH

et al. (2006) showed by flow microcalorimetry that interactions between Cd and pSi were mainly electrostatic, as the heat of adsorption was negligibly low [18]. Similarly, Pivovarov (2010) deduced exclusively electrostatic adsorption in the DDL, applying the Poisson-Boltzmann equation [17]. Single-injection experiments were carried out to study processes within 60 h (Fig. 4). After the injection of 50 mmol $Cu(NO_3)_2$ solution, the Cu concentration in the sample cell reached 2.74 mmol, and the Si concentration decreased by 0.67 mmol. The first peak in the thermogram (Fig. 4) reflects the enthalpy of mixing the $Cu(NO_3)_2$ solution. The increasing heat rate rapidly returned to the baseline and was subsequently stable for 5 h at -127.5 μJ s^{-1}. Then, it slowly increased to a maximum of -126.98 μJ s^{-1} until it fell back to the baseline after 25 h where it remained until the end of the experiment. However, these changes were very low and may not be attributed to Cu adsorption on pSi. More likely, polymerization/depolymerization of silicic acid caused the changes in heat rate. The decrease in Si concentration by 0.67 mmol altered the equilibrium between mSi and pSi. Thus, pSi dissolved, releasing mSi, until a new equilibrium was reached [4]. On the other hand, Cu^{2+} had a promoting effect on the polymerization of silicic acid [2]. This may also be the case in this experiment. Hence, the change in heat rate may be explained by the release of mSi from pSi induced by the change in total Si concentration or by the polycondensation of the pSi induced by Cu addition, or both.

Figure 5 summarizes possible processes of interactions between silicic acid and the metals depending on pH. The adsorption of divalent metal cations on deprotonated silanol groups of polymeric silicic acid can theoretically occur between pH 4 and 6. At more acidic pH, polymerization and deprotonation of silanol groups decreases, consequently decreasing the abundance of negative surface charge [4]. Moreover, mSi is uncharged under these conditions [7]. At circumneutral pH, silicic acid polymerization is at its maximum and the metals are predominantly present in their MeOH$^+$ state [7, 27]. Thus, they can be adsorbed on pSi or even may be complexed by deprotonated mSi. At undersaturation with respect to precipitation of silicates, divalent metal cations are incorporated into the polymeric network of silicic acid during its polymerization [2]. Moreover, metal cations favoured the polymerization of silicic acid and thus, promoted their own binding on negative surfaces of polymerizing and deprotonating silicic acid. At oversaturation, metal silicates are formed [19].

Here we show that chemical adsorption of divalent cations on pSi surfaces is a slow process not occurring within 24 h, at least under acidic pH and concentrations below those necessary for mineral precipitation, contradicting our working hypotheses. However, zeta-potential measurements revealed weak electrostatic interactions between the metals and pSi. Thus, the cations accumulate in the DDL, which may foster inner-sphere complexation over time.

4 Conclusion

We aimed to elucidate the extent and the mechanisms of the adsorption of Cd^{2+}, Cd^{2+}, and Pb^{2+} on pSi surfaces at pH 4–6 and ambient temperature. The interactions between the PTEs and silicic acid were mainly driven by electrostatic forces as revealed by zeta-potential measurements and may be explained by pure electrostatic adsorption in the diffuse double layer. The electrostatic interactions may be interpreted as the initial step of the interactions between Cd^{2+}, Cd^{2+}, and Pb^{2+} and (polymerizing) silicic acid, which were spectroscopically proven in long-term experiments. However, metal adsorption was not quantifiable in batch experiments so that our hypotheses had to be rejected. The results underline that processes of the interactions between the metals and Si phases are rather slow especially compared to the adsorption of the metals on other soil constituents like iron and aluminium oxides.

Data Availability The data underlying this article are available in the article.

Declarations

The work has not been published previously, is not under consideration for publication elsewhere, and the manuscript is approved by all authors. We know of no conflicts of interests associated with this publication.

Ethics Approval Not applicable.

Consent to Participate Not applicable.

Consent for Publication Not applicable.

Competing Interests The authors declare no competing interests.

References

1. Hayes F, Spurgeon DJ, Lofts S, Jones L (2018) Evidence based logic chains demonstrated multiple impact of trace metals on ecosystem services. J Environ Manage 223:150–164. https://doi.org/10.1016/j.jenvman.2018.05.053

2. Stein M, Georgiadis A, Gudat D, Rennert T (2020) Formation and properties of inorganic Si-contaminant compounds. Environ Pollut 265(B):115032. https://doi.org/10.1016/j.envpol.2020.115032

3. Wedepohl KH (1995) The composition of the continental crust. Geochem Cosmochim Acta 59:1217–1232. https://doi.org/10.1016/0016-7037(95)00038-2

4. Schaller J, Puppe D, Kaczorek D, Ellenbrock R, Sommer M (2021) Silicon cycling in soils revisited. Plants 10:295. https://doi.org/10.3390/plants10020295

5. Dietzel M (2000) Dissolution of silicates and the stability of polysilicic acid. Geochem Cosmochim Acta 64:3275–3281. https://doi.org/10.1016/S0016-7037(00)00426-9

6. Sommer M, Kaczorek D, Kuzyakov Y, Breuer J (2006) Silicon pools and fluxes in soils and landscapes - a review. J Plant Nutr Soil Sci 169:310–329. https://doi.org/10.1002/jpln.200521981

7. Bergna HE, Roberts, WO (eds) (2005) Colloidal Silica: Fundamentals and Applications (1st ed.). CRC Press, Boca Raton. https://doi.org/10.1201/9781420028706

8. Belton DJ, Deschaume O, Perry CC (2012) An overview of the fundamentals of the chemistry of silica with relevance to biosilification and technological advances. FEBS J 279:1710–1720

9. Veerhoff M, Brümmer GW (1993) Bildung schlecht kristalliner bis amorpher Verwitterungsprodukte in stark bis extrem versauerten Waldböden. Z. Pflanzenernähr. Bodenkd 56:11–17. https://doi.org/10.1002/jpln.19931560103

10. Dugger DL, Stanton JH, Irby BN, McConnell BL, Cummings WW, Maatman RW (1964) The exchange of twenty metal ions with the weakly acidic silanol group of silica gel. J Phys Chem 68:757–760. https://doi.org/10.1021/j100786a007

11. Kozawa A (1960) Ion-exchange adsorption of zinc and copper ions on silica. J Inorg Nucl Chem 21:315–324. https://doi.org/10.1016/0022-1902(61)80311-4

12. Schindler PW, Fürst B, Dick R, Wolf PO (1976) Ligand properties of surface silanol groups. I. Surface complex formation with Fe^{3+}, Cu^{2+}, Cd^{2+}, and Pb^{2+} J Colloid Interface Sci 55:469–475. https://doi.org/10.1016/0021-9797(76)90057-6

13. Mustafa S, Dilara B, Naeem A, Rehana N, Nargis K (2003) Temperature and pH effect on the sorption of divalent metal ions by silica gel. Adsorpt Sci Technol 21:297–307. https://doi.org/10.1260/026361703322405033

14. Ahrland S, Grenthe I, Norén B (1960) The ion exchange properties of silica gel I. The sorption of Na^+, Ca^{2+}, Ba^{2+}, UO_2^{2+}, Gd^{3+}, zr(IV) + nb, U(IV) and Pu(IV). Acta Chem 14:1059–1076

15. Xia K, Mehadi A, Taylor RW, Bleam WF (1997) X-ray absorption and electron paramagnetic resonance studies of Cu(II) sorbed to silica: surface-induced precipitation at low surface coverage. J Colloid Interface Sci 185:252–257. https://doi.org/10.1006/jcis.1996.4590

16. Bye GC, McEvoy M, Malatti MA (1982) Adsorption of copper (II) ions from aqueous solution by five silica samples. J Appl Chem Biotechnol 32:781–789. https://doi.org/10.1002/jctb.5030320714

17. Pivovarov S (2010) Diffuse sorption modeling: ionic adsorption on silica. J Colloid Interface Sci 352:158–162. https://doi.org/10.1016/j.jcis.2010.08.016

18. Lantenois S, Prélot B, Douillard JM, Szczodrowski K, Charbonnel MC (2006) Flow microcalorimetry: experimental development and application to adsorption of heavy metal cations on silica. Appl Surf Sci 253:5807–5813. https://doi.org/10.1016/j.apsusc.2006.12.064

19. Yates DM, Joyce KJ, Heaney PJ (1998) Complexation of copper with polymeric silica in aqueous solution. Geochim Cosmochim Acta 13:235–241. https://doi.org/10.1016/S0883-2927(97)00062-0

20. Stein M, Georgiadis A, Ingwersen J, Rennert T (2021) Does silica addition affect translocation and leaching of cadmium and copper in soil? Environ. Poll 288:117738. https://doi.org/10.1016/j.envpol.2021.117738

21. Prozeller D, Morsbach S, Landfester K (2019) Isothermal titration calorimetry as a complementary method for investigating nanoparticle-protein interactions. Nanoscale 11:19265–19273. https://doi.org/10.1039/C9NR05790K

22. Ellerbrock R, Stein M, Schaller J (2022) Comparing amorphous silica, shored-range-ordered silicates and silicic acid species with FTIR. Sci Rep 12:11708. https://doi.org/10.1038/s41598-022-15882-4

23. Zhi K, Wang L, Zhang Y, Jiang Y, Zhang L, Yasin A (2018) Influence of size and shape of silica supports on the sol–gel surface molecularly imprinted polymers for selective adsorption of gossypol. Materials 11(5):777. https://doi.org/10.3390/ma11050777

24. Xu P, Wang H, Tong R, Du Q, Zhong W (2006) Preparation and morphology of SiO2/PMMA nanohybrids by microemulsion polymerization. Colloid Polym Sci 284:755–762. https://doi.org/10.1007/s00396-005-1428-9

25. Sikora A, Shard AG, Minelli C (2016) Size and ζ-potential measurement of silica nanoparticles in serum using tunable resistive pulse sensing. Langmuir 32:2216–2224. https://doi.org/10.1021/acs.langmuir.5b04160

26. Chuan MC, Shu GY, Liu JC (1996) Solubility of heavy metals in a contaminated soil: Effects of redox potential and pH. Wat Air and Soil Poll 90:543–556. https://doi.org/10.1007/bf00282668

27. Spark KM, Johnson BB, Wells JD (1995) Characterizing heavy metal adsorption on oxides and oxyhydroxides. Eur J Soil Sci 46:621–631. https://doi.org/10.1111/j.1365-2389.1995.tb01358.x

28. Gustafsson JP (2013) Visual MINTEQ Visual MINTEQ - a free equilibrium speciation model. http://vminteq.lwr.kth.se/. Accessed 31 May 2017

29. Ziyath A, Mahbub P, Goonetilleke A, Adebajo M, Kokot S, Oloyede A (2011) Influence of physical and chemical parameters on the treatment of heavy metals in polluted stormwater using zeolite - A review. Water Resour Prot 3:758–767. https://doi.org/10.4236/jwarp.2011.310086

30. Colic M, Fisher ML, Franks GV (1998) Influence of ion size on short-range repulsive forces between silica surfaces. Langmuir 14:6107–6112. https://doi.org/10.1021/la980489y

31. Zataka D, Radian A, Mishael YG (2011) Applying zeta potential measurements to characterize the adsorption on montmorillonite of organic cations as monomers, micelles, or polymers. J Colloid Interface Sci 352:171–177. https://doi.org/10.1016/j.jcis.2010.08.010

32. Kirby BJ, Hasselbrink EF Jr (2004) Zeta potential of microfluidic substrates: 1. Theory, experimental techniques, and effects on separations. Electrophoresis 25:187–202. https://doi.org/10.1002/elps.200305754

33. Juang RS, Wu WL (2002) Adsorption of sulfate and copper(II) on goethite in relation to the changes of zeta potentials. J Colloid Interface Sci 249:22–29. https://doi.org/10.1006/jcis.2002.8240

34. Erdemoğlu M, Sarikaya M (2006) Effects of heavy metals and oxalate on the zeta potential of magnetite. J Colloid Interface Sci 300:795–804. https://doi.org/10.1016/j.jcis.2006.04.004

35. Ostolska I, Wiśniewska M (2014) Application of the zeta potential measurements to explanation of colloidal Cr2O3 stability mechanism in the presence of the ionic polyamino acids. Colloid Polym Sci 292:2453–2464. https://doi.org/10.1007/s00396-014-3276-y